ARTICLE

OBC
www.rsc.org/obc

Mutual induced fit in cyclodextrin–rocuronium complexes

Alan Cooper,[a] Margaret Nutley,[a] Elizabeth J. MacLean,[b] Ken Cameron,[c] Lee Fielding,[c] Jordi Mestres†[c] and Ronald Palin*[c]

[a] *Department of Chemistry, Glasgow University, Glasgow, Scotland, UK G12 8QQ*
[b] *CCLRC Daresbury Laboratory, Warrington, Cheshire, UK WA4 4AD*
[c] *Department of Chemistry, Organon Research, Newhouse, Scotland, UK ML1 5SH. E-mail: r.palin@organon.co.uk*

Received 15th October 2004, Accepted 3rd March 2005
First published as an Advance Article on the web 23rd March 2005

The binding of rocuronium bromide to 6-perdeoxy-6-per(4-carboxyphenyl)thio-γ-cyclodextrin sodium salt, displays biphasic behaviour characteristic of the formation of a binary and 2 : 1 ternary guest–host complex in aqueous solution. Thermodynamic and structural data on this sequential complexation process can be rationalised within a single model involving switching of the conformational equilibria of both the rocuronium bromide and cyclodextrin molecules. Isothermal titration calorimetry (ITC), NMR and fluorescence experiments in solution, together with X-ray crystallography and molecular modelling, suggest that in order to induce encapsulation both rocuronium bromide and the modified cyclodextrin undergo conformational changes. Ring A of rocuronium bromide 'switches' from the more sterically encumbered chair to the sterically less demanding twist–boat, whilst the modified cyclodextrin "opens" its cavity to allow the steroid to enter. The recognition and mutual induced fit between cyclodextrin and steroid represents a classic example of dynamic host–guest chemistry.

Introduction

Neuromuscular blocking agents (NMBAs, also known as muscle relaxants) are extensively used during surgical procedures to produce complete relaxation of skeletal muscle,[1–3] usually by blocking the nicotinic acetylcholine receptor.[4] The reversal of this neuromuscular block (NMB) at the end of surgery is often necessary to speed up the recovery of a patient's muscle function and to prevent residual muscle paralysis.[5,6] All reversal agents used in anaesthetic practice to date exert their action by inhibiting acetylcholine esterase, effectively increasing the concentration of acetylcholine at the neuromuscular junction, leading to displacement of the NMBA from the receptor site and thereby re-establishing muscle function.[7,8] Unfortunately this mechanism of action has the inherent disadvantage of nonselective activation of the muscarinic acetylcholine receptors leading to undesirable side effects, for example bradycardia, hypotension and bronchoconstriction.[9] Recently, a radically different approach to reverse NMB by complex formation between the NMBA and host molecules such as cyclodextrins and cyclophanes has been developed.[10] In particular, a number of cyclodextrin derivatives[11,12] have been designed as drug entities to form tight complexes with rocuronium bromide (Esmeron™ **1**), one of the most widely used NMBAs in surgery.

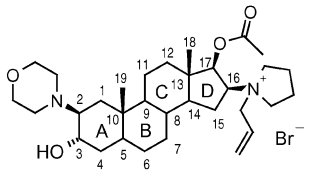

1

Cyclodextrins have been used by the pharmaceutical industry for many years as excipients to improve water solubility, stability and bioavailability of lipophilic drugs.[13] The cyclic nature of these oligosaccharides, comprising different numbers of glucose units (α, 6; β, 7; γ, 8), defines a hydrophobic cavity able to accommodate a wide range of non-polar molecules. The binding affinities, selectivities and other properties can be attenuated by functional group modification of the side chains attached to primary or secondary hydroxyl groups faces of the cyclodextrin torus. We have demonstrated the importance of the hydrophobic cavity within this series of cyclodextrins in the formation of complexes, by the fact that the extended cavities of the persubstituted γ-cyclodextrin derivatives are more potent than the corresponding monosubstituted analogs.[12] Charged substituents at the rim of the cyclodextrin cavity seem to contribute to the reversal activity by electrostatic interactions with the quaternary nitrogen of **1**. This is borne out by the observation that the corresponding neutral hydroxyl derivatives are less potent.[12] Consistent with this chelation mechanism of action, one of these derivatives, 6-perdeoxy-6-per(2-carboxyethyl)thio-γ-cyclodextrin sodium salt (**2**), forms a high affinity binary complex (association constant, K_a *ca.* 10^7 M^{-1}), as determined by isothermal titration calorimetry (ITC).[14] This reduces the occupancy of NMBA at the nicotinic acetylcholine receptors allowing restoration of muscle function. Cyclodextrin **2** causes rapid reversal of NMB and appears to be superior to current clinically used reversal agents in terms of efficacy and side effects[15] and is presently being evaluated in clinical trials.

Amongst a range of other modified γ-cyclodextrins examined, we have also reported on, 6-perdeoxy-6-per(4-carboxyphenyl)thio-γ-cyclodextrin sodium salt (**3**), which, in contrast to **2** and most other variants, demonstrates unusual biphasic binding with **1**.[16] Such complicated titration behaviour might arise for a number of reasons including multiple binding sites, ligand-induced aggregation to form higher-stoichiometery complexes, conformational switches in the [**3**–**1**] complex, or indeed a combination of such effects.

Here we present thermodynamic and structural data from a variety of sources using ITC, UV absorbance and fluorescence, X-ray crystallography and NMR which, together with theoretical calculations, aim to characterise and rationalise the nature of this binding process. The consensus arising from this wide-ranging experimental and theoretical approach is that the biphasic nature of [**3**–**1**] complexation arises from a stepwise addition of **1** to the modified cyclodextrin **3**, to form a non-covalent 2 : 1 ternary guest–host complex involving conformational switches in both **1** and **3**.

† Present address: Chemogenomics Laboratory, Research Group on Biomedical Informatics (GRIB), Institut Municipal d'Investigació Mèdica & Universitat Pompeu Fabra, Passeig Marítim de la Barceloneta 37–49, 08003 Barcelona (Catalonia), Spain.

DOI: 10.1039/b415903a

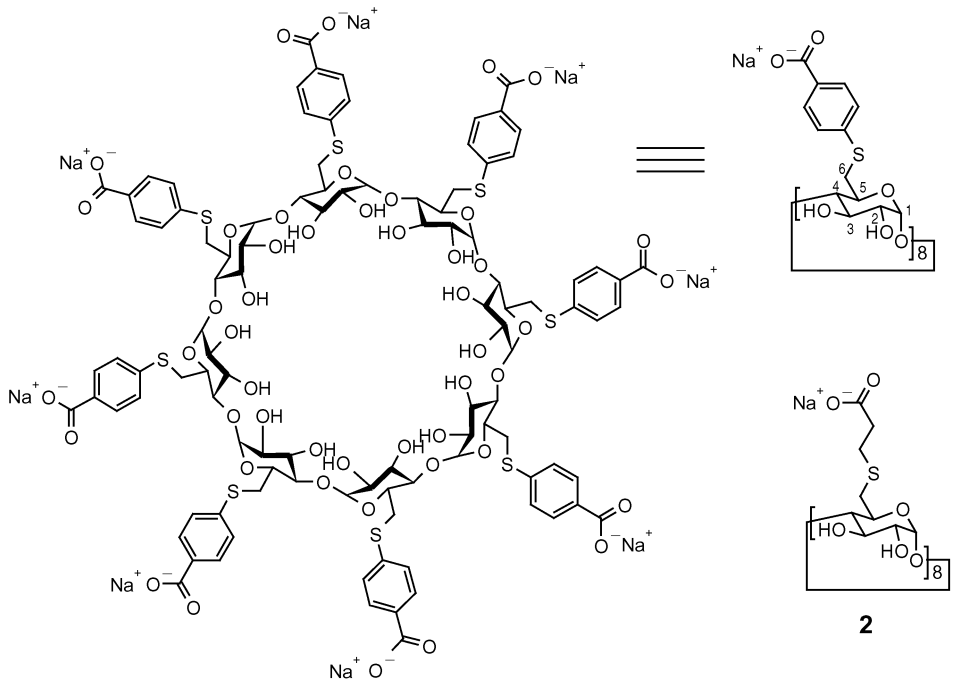

Results

ITC

Isothermal titration microcalorimetry experiments on the binding of **1** to **3** show a pattern of binding isotherms that is inconsistent with simple 1 : 1 complexation (Fig. 1 and Fig. 2). Typically the calorimetric isotherms are biphasic, showing endothermic heat pulses for initial injections, becoming exothermic with later additions, though the actual thermogram shapes are very temperature dependent. This complicated pattern is seen regardless of whether the calorimetric titration is done by addition of **1** ("ligand") to the cyclodextrin, or *vice versa* (Fig. 2). Similar biphasic behaviour is seen with other steroidal NMBAs binding to this cyclodextrin (vecuronium: data not shown) but not for the same ligands binding to other modified cyclodextrins (*e.g.* **2**, see Fig. 1a).[14,16] The same effects are seen using 10-fold lower cyclodextrin concentrations, and this seems to rule out any aggregation behaviour that might otherwise explain biphasic thermograms.[17,18] Separate experiments (unpublished) show no chemical decomposition of rocuronium bromide or cyclodextrins under these conditions.

All these data fit consistently with a sequential two-site binding model in which relatively tight binding of one rocuronium bromide to **3** is followed (at higher concentrations) by weaker association with a second molecule of **1**.

$$3 + 1 \overset{K_1,\Delta H_1}{\rightleftharpoons} [3.1] + 1 \overset{K_2,\Delta H_2}{\rightleftharpoons} [3.1.1]$$

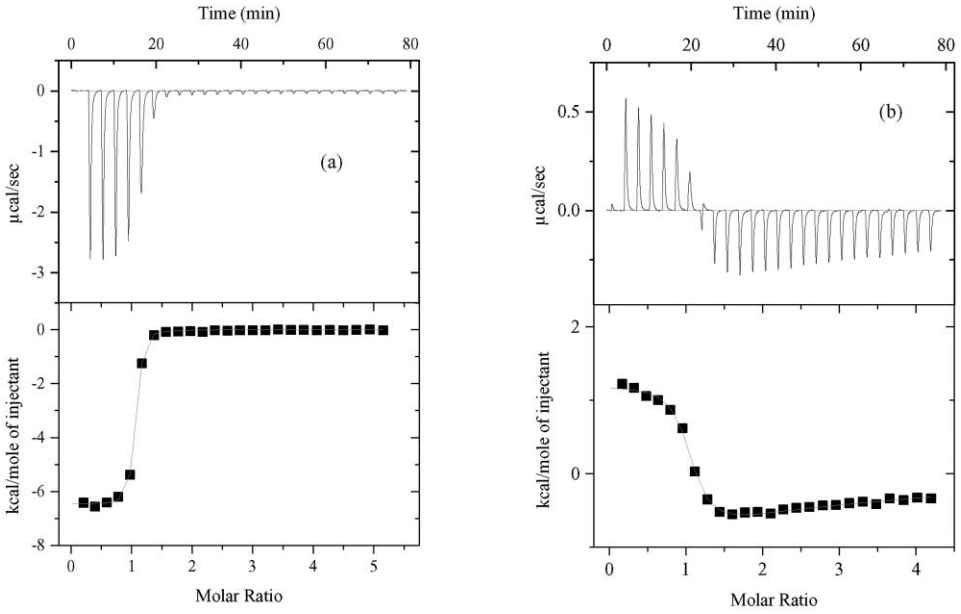

Fig. 1 Examples of single-site and biphasic ITC data for binding of rocuronium bromide (**1**) to modified γ-cyclodextrins (**2** and **3**) at 25 °C, in 50 mM phosphate buffer, pH 7: (a) 25 × 10 µL additions of **1** (1.32 mM) to **2** (0.05 mM); (b) 25 × 10 µL additions of **1** (1.57 mM) to **3** (0.073 mM). The solid lines (lower panels) show the non-linear regression fits to: (a) a single-site binding model, with $N = 0.99$, $K = 9.4 \times 10^6$ M^{-1}, $\Delta H = -6.5$ kcal mol^{-1}, and (b) a sequential two-site binding model with parameters given in Table 1 (1 cal = 4.184 J).

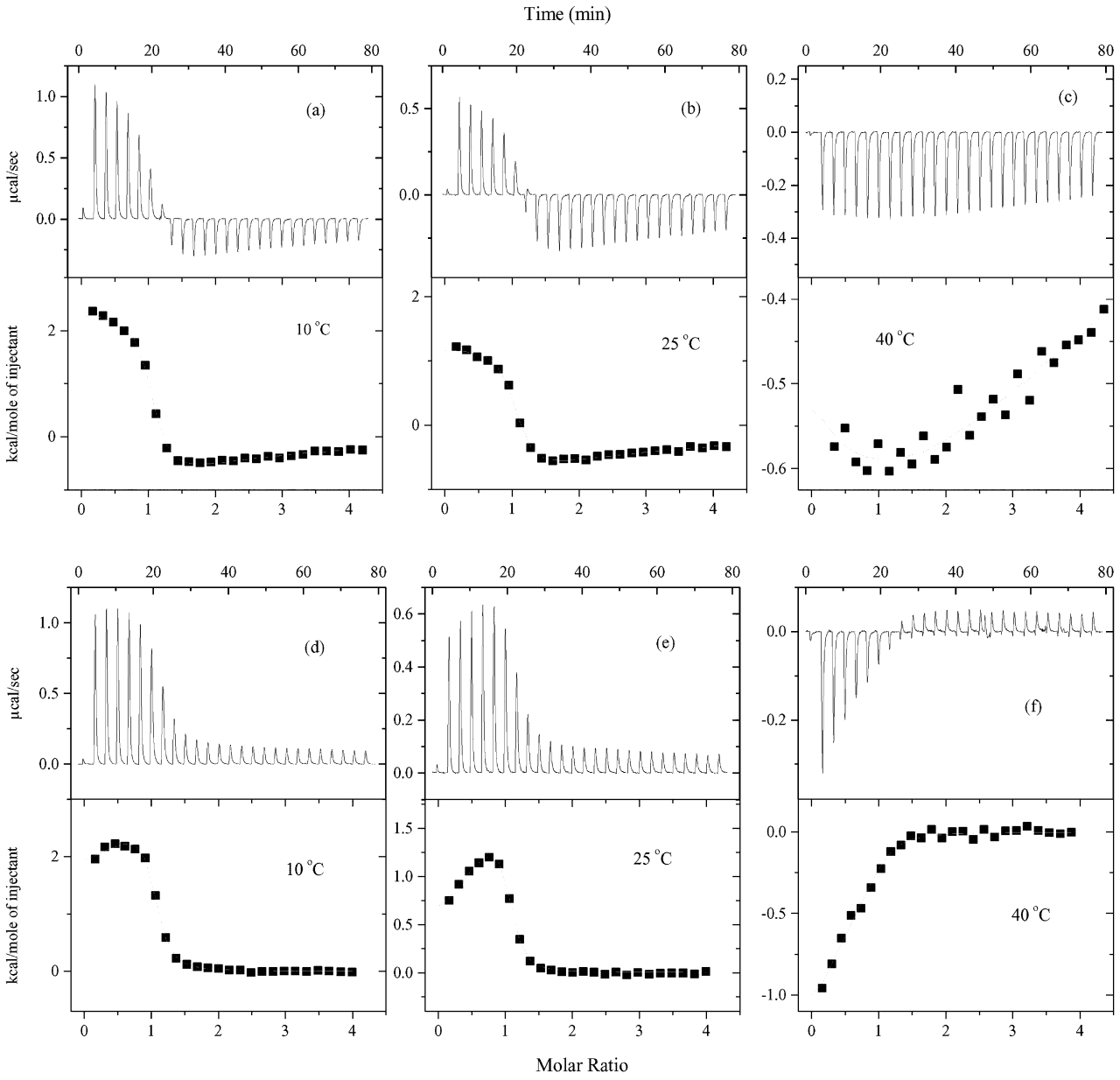

Fig. 2 Representative ITC data showing the characteristic biphasic binding behaviour of [**3**–**1**] over a range of temperatures (10, 25 and 40 °C), with injections of **1** into **3** (a–c) or **3** into **1** (d–f). In all cases the differential binding curves (solid lines, lower panels) fit consistently to a sequential two-site binding model (2 : 1 rocuronium bromide–cyclodextrin) with thermodynamic parameters given in Table 1.

Globally consistent thermodynamic parameters for this sequential binding scheme are shown in Table 1.

Although the data fit consistently over a wide temperature range, the apparent enthalpies of binding to the two sites also show an unusual temperature dependency for a system of this kind (Fig. 3).

Small decreases in binding enthalpies with increasing temperature (ΔC_p effects), such as is seen in the case of [**2**–**1**] (Fig. 3), are typical of hydrophobic and other weak cooperative interactions in solution.[19,20] However, the much larger temperature variations in ΔH observed for both sites in [**3**–**1**] complexes are atypical, indicating a more specific effect of temperature on the binding mechanism(s).

UV/fluorescence

Cyclodextrin **3** has a typical aromatic near-UV absorbance spectrum (λ_{max} = 277 nm), which shifts slightly on addition of **1** (Fig. 4, upper panel). Fluorescence spectra show much larger changes, where **3** gives a broad fluorescence emission

Table 1 Thermodynamic parameters for [**3**–**1**] binding at different temperatures derived by fitting experimental ITC data to a two-site sequential binding model (estimated standard deviation in parentheses) (1 cal = 4.184 J)

T/°C	$K_1/10^6$ M^{-1}	ΔH_1/kcal mol^{-1}	ΔS_1 cal mol^{-1} K^{-1}	$K_2/10^3$ M^{-1}	ΔH_2/kcal mol^{-1}	ΔS_2 cal mol^{-1} K^{-1}
10	1.3 (0.3)	2.28 (0.05)	+36 (1)	4.0 (1.5)	−3.1 (0.3)	+5.5 (2)
25	1.4 (0.2)	1.20 (0.05)	+31 (1)	2.0 (0.5)	−5.3 (0.1)	−3 (1)
32	1.1 (0.3)	0.43 (0.02)	+29 (1)	1.5 (0.3)	−6.9 (0.9)	−8 (3)
35	0.9 (0.2)	0.10 (0.01)	+28 (1)	1.3 (0.17)	−7.7 (0.7)	−11 (3)
40	0.35 (0.03)	−0.65 (0.02)	+23 (1)	0.7 (0.1)	−9 (2)	−16 (6)

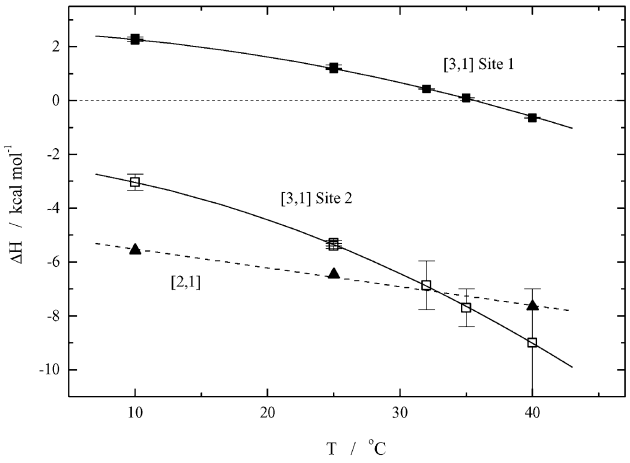

Fig. 3 Temperature dependencies of enthalpies of binding of rocuronium bromide (**1**) to modified cyclodextrins **2** (solid triangles, ▲) and **3** (site 1-solid squares, ■; site 2-open squares, □). Linear regression of data for [**2**–**1**] gives $\Delta C_p = -69.7$ (± 5.6) cal K^{-1} mol^{-1}. Curves through [**3**–**1**] data (both sites) correspond to theoretical behaviour based on the conformational switch model (see text) with parameters listed in Table 2.

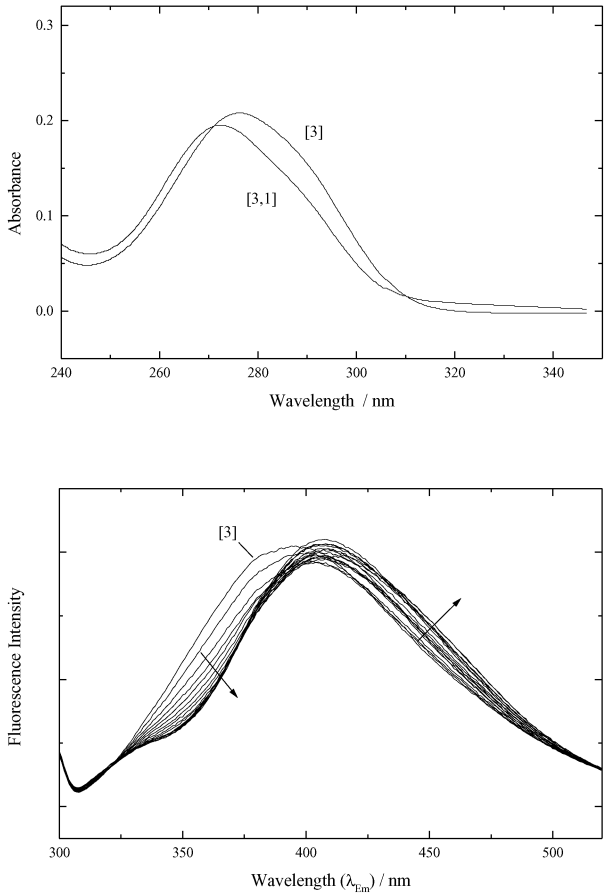

Fig. 4 Changes in UV absorbance and fluorescence of cyclodextrin (**3**) upon addition of rocuronium bromide(**1**). *Upper panel*: UV absorbance spectra of **3** in solution (≈ 2 μM, pH 7.4, 25 °C) in the presence ([**3**–**1**]) and absence ([**3**]) of excess **1**. *Lower panel*: fluorescence emission spectra of **3** in solution (2 μM, $\lambda_{exc} = 270$ nm) in the presence of increasing concentrations of **1**. The initial spectrum of **3** alone (labelled[3]) shows progressive decrease in intensity around 360 nm on addition of low concentrations of **1**, followed by subsequent increase at longer wavelengths upon addition of higher concentrations of **1** (**1** alone does not fluoresce under these conditions.) The arrows indicate the direction of increasing **1** concentration (0.2–100 μM, as in Fig. 5).

spectrum ($\lambda_{em} = 390$ nm) when excited at 270 nm which changes significantly upon addition of **1** (Fig. 4, lower panel). These changes are also biphasic. Low concentrations of **1** produce a decrease in cyclodextrin fluorescence intensity at shorter wavelengths (*ca.* 360 nm) that saturates after addition of about one equivalent. Subsequent additions of higher concentrations of **1** give rise to a more gradual fluorescence red-shift and increase in intensity.

These fluorescence changes can be analysed to give estimates of the apparent binding affinity of **1** for **3**, with results that are comparable to those obtained more directly from ITC data (Fig. 5).

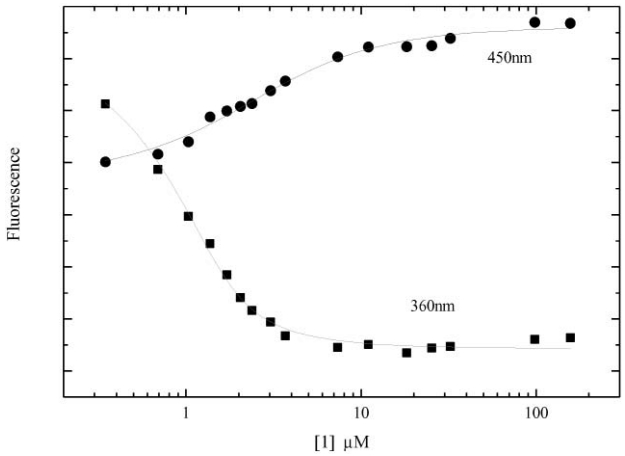

Fig. 5 Fluorescence intensity changes at 360 and 450 nm upon addition of **1** to **3** in solution (2 μM) at 25 °C. The lines are theoretical fits for binding to the high- and low-affinity sites, respectively.

At low concentrations of **1** the fluorescence titration curve fits well to a single-site binding model with $K_a \approx 6 \times 10^6$ M^{-1}. The higher concentration data are consistent with a second (subsequent) binding affinity at least one order of magnitude weaker. This observation of an apparent biphasic binding behaviour at cyclodextrin concentrations up to 50-fold lower than in the ITC experiments further suggests that these effects are not due to aggregation.‡

NMR

All of the signals at 30 °C in the ^{1}H NMR (D_2O) spectrum of the per-6-substituted cyclodextrin **3** are very broad.[16] The addition of the guest steroid **1** results in a dramatic sharpening of the signals of **3** and some slight broadening of the signals of **1** (Fig. 6).[16] The sharpening of the cyclodextrin signals indicates that the dynamic averaging process occurring in **3** has been interrupted by the entry of the guest steroid. The general broadening in the ^{1}H spectrum of **1** is an indication of reduced molecular motion of the complexed steroid. Steroids such as **1** are not completely rigid and there is some conformational freedom at both the ring A and the ring D ends of the molecule. The increase in line width on going from free steroid to bound steroid is analogous to that induced by cooling, which moves the normally fast rate of conformational averaging into the slow exchange regime. It can be seen that in the complex the 18-methyl signal is broader than that from the 19-methyl. This is probably due to restricted rotation of the bulky 16β-quaternary pyrrolidine and 17β-ester groups. Therefore, it appears that the tight binding of **1** in the cyclodextrin cavity reduces the conformational flexibility of the steroid.

The nature of the dynamics in empty **3** was investigated by variable temperature ^{1}H NMR. Heating of **3** to 80 °C resulted

‡ We are grateful to an anonymous referee for pointing out that π–π charge transfer interactions between adjacent phenyl groups in **3** might possibly explain the relatively large fluorescence Stokes shift seen here (Fig. 4), although we have no other evidence to support such a mechanism at this stage.

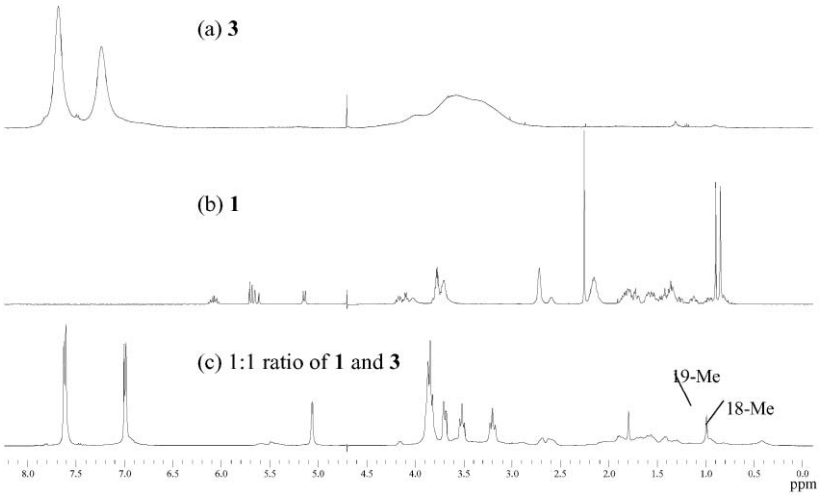

Fig. 6 ^{1}H NMR spectra of (a) 5 mM **3**, (b) 1 mM **1** and (c) a 1 : 1 mixture of **1** and **3** at 30 °C in pH 7.5 phosphate buffered D_2O. The spectrum of **3** is characteristic of a molecule that is converting on the NMR time scale between different conformations (intermediate exchange). The spectrum of **1** is normal for a small molecule in solution. In the equimolar mixture the spectrum of **3** sharpens markedly and the steroid signals broaden slightly and move to new chemical shifts, indicating **1** is in a different environment.

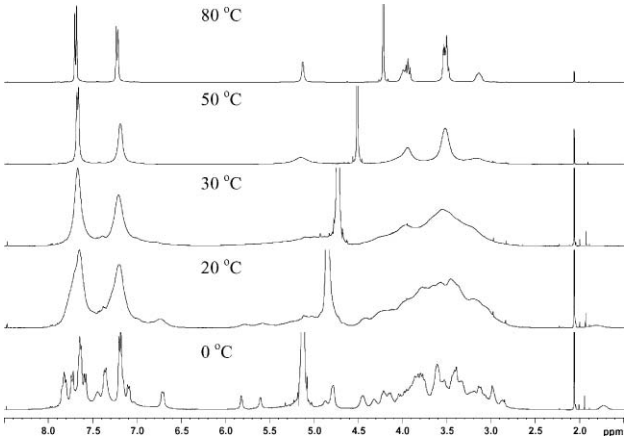

Fig. 7 Temperature dependence of the 400 MHz ^{1}H NMR spectra of uncomplexed **3** in D_2O. The low temperature spectrum corresponds to an asymmetric low energy conformation of the cyclodextrin. The high temperature spectrum is the averaged spectrum of multiple cyclodextrin conformations.

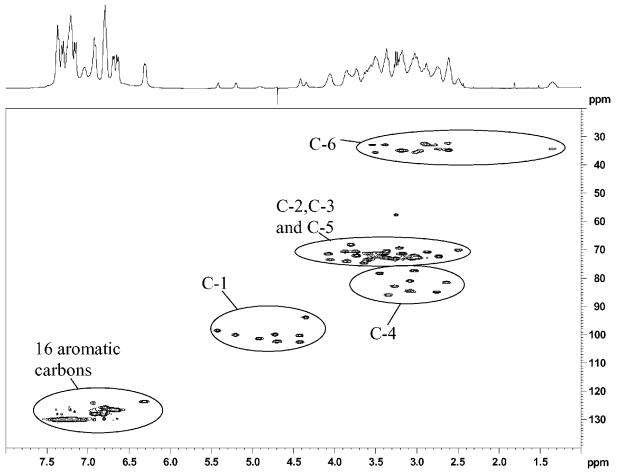

Fig. 8 HSQC ^{13}C–^{1}H correlation NMR spectrum of **3** at 0 °C in D_2O. This spectrum reveals a correlation for each unique C–H unit and suggests (no other peaks detected) just one major low energy conformation.

in a sharpening of the signals and cooling to just 0 °C resulted in a decoalescence of the signals into multiple signals (Fig. 7).

The 0 °C 2D C–H correlation spectrum of **3** reveals unique signals from each glucosyl residue of the cyclodextrin (Fig. 8). This is most obvious for the anomeric carbon (C-1), where eight distinct cross-peaks can be seen in the region δ 1_H 4.65–5.85 ppm and δ 13_C 92–102 ppm and in the region of the C-4 correlations (δ 1_H 3.0–3.9 ppm and δ 13_C 77–86 ppm), where, again, eight distinct cross peaks appear (see **1** for atom labelling). Multiple cross peaks also occur in the C-6 region and in the C-2, C-3, C-5 regions. Although the signals have not all been assigned, it is clear that **3** is asymmetric at low temperatures and that each glucosyl residue now has a unique set of chemical shifts. This proves that the simplicity (degeneracy) of the room temperature spectrum is due to fast motional averaging in a dynamic cyclodextrin molecule and is not an indication of a well ordered symmetric molecule.

Although, in principle, it should be possible to determine ligand binding parameters from such spectra (Fig. 6), ^{1}H NMR can only reliably measure association constants up to *ca.* 10^4–10^5 M^{-1}. Therefore, it is not feasible to use NMR under the present conditions to determine K_a for the first binding step seen here ($K_a \sim 1 \times 10^6$ M^{-1}). However, we have recently reported the association constant K_a for the second binding site (using a curve fitting method[21]) at 1340 M^{-1} which is consistent with ITC data (Table 1).[16]

Crystallography

6-Perdeoxy-6-per(4-carboxyphenyl)thio-γ-cyclodextrin sodium salt. The solid-state crystal structure of **3** is highly ordered and there are eight π–π stacking interactions between the phenyl rings of the cyclodextrin side chains (Fig. 9) in the C_4-symmetric structure. The tendancy of π–π interactions is to adopt preferably two types of stacking: offset and T-shaped.[22] Both types of interaction are observed in the crystal structure of **3** and, of the eight π–π interactions present, four are of the offset type and four of the T-shaped type.

6-Perdeoxy-6-per(4-carboxyphenyl)thio-γ-cyclodextrin sodium salt-rocuronium bromide complex. The solid-state structure of the [**3**–**1**] complex is much less ordered than the corresponding free **3** crystal structure (Fig. 9). An interesting feature of the [**3**–**1**] complex crystal structure is that the asymmetric unit contains two distinct [**3**–**1**] complexes. Upon close inspection of the structure, it can be seen that **1** presents different conformations of the A ring of the steroidal core. Most interestingly, both chair and twist–boat conformations exist in one crystal structure of the complex with the side chains in the cyclodextrin having

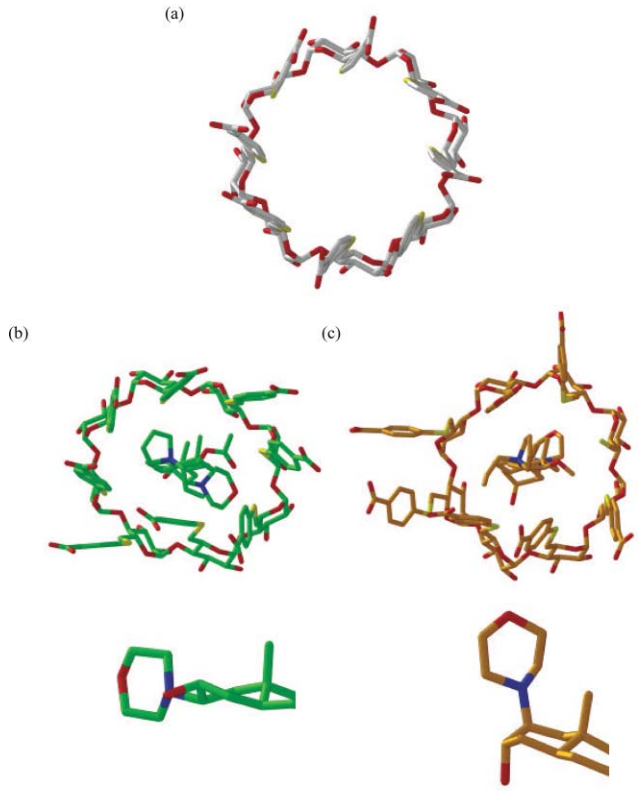

Fig. 9 Crystal structures of **3** and the two independent [**3**–**1**] complexes:§ (a) symmetrical crystal structure of **3** alone, (b) crystal structure of the [**3**–**1**] complex with ring A of **1** in the twist–boat conformation, (c) crystal structure of the [**3**–**1**] complex with ring A of **1** in the chair conformation.

to adapt their conformations to accommodate the different conformations of the steroidal structure of **1** (Fig. 9).

In summary, the experimental data so far point to the following general conclusions:

(1) ITC, fluorescence and NMR data show that **1** and **3** can form a ternary 2 : 1 complex in solution in a sequential binding mechanism involving initial tight binding of one molecule of **1** ($K_a \sim 10^6$ M^{-1}) followed, at higher concentrations, by addition of a second molecule of **1** ($K_a \sim 10^3$ M^{-1}).

(2) Both binding steps show unusual temperature dependence in heats of binding (ITC): step 1 initially endothermic and both becoming progressively more exothermic with increases in temperature.

(3) Structural studies both in solution and solid-state (NMR, crystallography) show that both **1** and **3** display significant conformational flexibility. Crystals of 1 : 1 complexes (presumably representing the tight-binding complex seen in solution) show two different conformations of rocuronium bromide in adjacent cyclodextrin cavities.

Discussion

The challenge at this point is to rationalize the initial endothermic step observed from ITC experiments by making use of all the structural and binding data obtained experimentally from X-ray crystallography, NMR, and UV/fluorescence to arrive at a plausible hypothesis regarding the molecular recognition between the cyclodextrin and **1**. It will be assumed that the major source of the temperature variation in apparent binding enthalpy, observed by ITC, arises from thermal isomerisation equilibrium of either the cyclodextrin or **1**, or possibly even both.

The conformations of ring A in steroidal NMBAs have been studied for many years.[23–25] ^{1}H NMR studies of **1**[26] and an analoguous steroid[27,28] have demonstrated conclusively that ring A exists in solution in a dynamic equilibrium between both chair and twist–boat forms (see Fig. 9). The energy difference between the chair and the twist–boat conformations of ring A is relatively small (*ca.* ±1 kcal mol^{-1}) and the fraction of each form present in solution can be easily altered by merely changing the solvent.[27,28] However, only chair conformations of ring A *trans*-2β-amino-3α-ols have been seen in solid-state studies. For instance, the ring A chair is seen in the crystal structure of the model compound, 3α,12β-dihydroxy-2β-morpholino-5α-pregnan-20-one (**4**),[29] and in the recent X-ray study of **1** encapsulated as a cyclodextrin complex within **2**.[14] The observation of both chair and twist–boat conformations in the same crystal structure is a dramatic illustration of the almost equal stabilities of chair and twist–boat ring A forms.

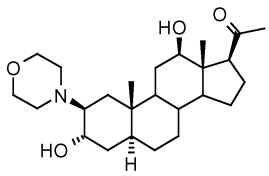

4

The facile interchange between a chair and a twist–boat conformation in ring A of **1** is potentially a key factor in the formation of the [**3**–**1**] complex. The *trans*-axial substituents on ring A and the pseudo *trans*-axial substituents on ring D make the steroidal structure of **1** too bulky to enter into the cavity of a γ-cyclodextrin, even when considering the possibility of a certain degree of conformational adaptation of the cyclodextrin during the entry of **1**. However, adoption of a twist–boat conformation in ring A allows the profile of **1** to flatten and, thus, eases the entry of **1** into the cyclodextrin cavity. In addition, it should be noted that the hydrophobic environment of the cyclodextrin core would be expected to further stabilise the twist–boat conformation during its passage. This follows from the rise in population of the twist–boat form in the presence of hydrophobic solvents.[27,28] Upon emerging at the secondary hydroxyls of the cyclodextrin, the more hydrophilic environment and the contact with the aqueous medium would be expected to destabilise the twist–boat conformation in favour of the chair conformation and the molecule will tend to revert back into a chair conformation. The chair conformation will then lock the steroid into the cyclodextrin in a manner similar to the formation of rotaxanes.

The X-ray structure of **3** has been determined and it shows an axially C_4-symmetrical cyclodextrin with all the aromatic rings of the side chain in a regular π-stacked arrangement (see Fig. 9).

However, the classical picture of a truncated-cone shaped cyclodextrin with a symmetrical cavity, although often used, can be misleading. X-ray crystallography shows that γ-cyclodextrin adopts a slightly elliptical structure resulting in the cavity not being perfectly octagonal.[30,31] In addition, the study of γ-cyclodextrin by neutron diffraction at −163 °C has shown that the glucose residues are linked by quite disparate torsion angles and that one of the glucose units has a large deviation from the ideal chair conformation.[32] Hence, asymmetry is a normal condition for γ-cyclodextrins. The asymmetry of cyclodextrins appears to be more pronounced when they are substituted. The X-ray structure of per-(2,3,6-tri-*O*-methyl)-γ-cyclodextrin has two glucosyl residues rotated *ca.* 180°, resulting in bowl shaped molecules.[33] There is overwhelming evidence from NMR that cyclodextrins are flexible molecules that adapt their conformation to accommodate different shaped guests.[34]

§ CCDC reference numbers 253402 and 253403. See http://www.rsc.org/suppdata/ob/b4/b415903a/ for crystallographic data in CIF or other electronic format.

This is a somewhat different picture to the rigid truncated-cone structure that is often depicted by X-ray studies.

Self-complexation of the carboxybenzyl group in **3** is a possible cause of the dynamic effects and the asymmetry observed in the ^{1}H and ^{13}C NMR spectra. However, the chain length at the six position of **3** (CH_2–S–Ar) is not long enough for the phenyl ring to be threaded through the cavity so that the carboxylate can protrude out of the hydrophobic cavity and into the aqueous solvent. The polar carboxylate group would not be stable in the hydrophobic cavity of the cyclodextrin. Therefore, self-complexation would require a significant distortion of the cyclodextrin, which would result in **3** being highly unsymmetric and so explain the observed low temperature NMR spectra (Fig. 7).

Upon addition of **1**, the conformation of **3** will adapt by induced fit to the structure of **1**. This conformational adaptation of the host can be experimentally observed when comparing the UV spectra of the free host and the host–guest complex (see Fig. 4). The shift in absorbance in the UV spectrum of **3** on addition of **1** is reminiscent of the hypochromic shifts seen upon unstacking of DNA base pairs. This may reflect similar changes in the phenyl ring stacking around the **3** torus and/or the insertion of a phenyl ring into the cavity.

One should expect that the tight fit of **1** in the cyclodextrin cavity does not allow significant changes in the glucosyl ring conformation. In fact, the X-ray structure of the [**3**–**1**] complex shows that the cavity is elliptical and so is unsymmetrical (see Fig. 9). The ^{1}H NMR spectrum of the complex at 30 °C shows the cyclodextrin resonances to be sharp, with only one resonance for each of the eight glucosyl protons (Fig. 6). This indicates that, in solution, the complex is in a fast dynamic equilibrium. At the same time, **1** can reorientate within the cavity (possibly by rotation) so that the electrostatic interaction of the quaternary nitrogen is shared over all eight carboxylate groups of **3**. This may also be in fast exchange between bound and free states.

On the basis of all these experimental observations, a simple hypothesis for the binding of **1** to **3** (and vice versa) can be put forward. This hypothesis assumes that, although in the solid-state at low temperatures **3** exists in a highly ordered single conformation where the pendant aryl side-chains are held together by an ensemble of eight π–π stacking interactions, this highly ordered π-stacking arrangement is not necessarily retained in solution. Freed from the constraints imposed by crystal packing, **3** exists in more disordered forms with the π–π stacking interactions due to the self complexation of one of the carboxybenzyl groups. In the ordered ("closed") form, the entry of **1** into the cavity of the cyclodextrin would be relatively difficult compared to the easier access afforded in a more disordered ("open") conformational ensemble in solution.

The expulsion of the carboxyphenyl group would require a certain amount of energy, providing a plausible explanation for the endothermic step observed in ITC experiments and being consistent with both NMR and UV/fluorescence experiments. Also, ITC experiments show a temperature dependence of the binding, consistent with the fact that at higher temperatures the population of disordered forms will increase, allowing an easier entry of **1** into the cyclodextrin cavity.

The arguments exposed above can be modelled using a simple isomerisation scheme. Let us assume A and B are representative forms of the ensemble of disordered and ordered conformations, respectively, that **3** can adopt in equilibrium.

$$\mathrm{A} \rightleftharpoons \mathrm{B};\ \Delta H_{\mathrm{AB}};\ K_{\mathrm{AB}} = [\mathrm{B}]/[\mathrm{A}]$$

with only isomer A being able to form a complex (A–L) with **1** (ligand L):

$$\mathrm{A} + \mathrm{L} \rightleftharpoons \mathrm{A\text{–}L};\ \Delta H_0;\ K_0 = [\mathrm{A\text{–}L}]/[\mathrm{A}][\mathrm{L}]$$
$$\Delta G_0{}^{0} = -RT.\ln K_0 = \Delta H_0 - T.\Delta S_0{}^{0}$$

The observed (apparent) association constant in any experiment involving such shifts in isomer equilibrium is given by:

$$\begin{aligned} K_{\mathrm{obs}} &= [\mathrm{A\text{–}L}]/\{([\mathrm{A}] + [\mathrm{B}])[\mathrm{L}]\} \\ &= [\mathrm{A\text{–}L}]/\{(1 + [\mathrm{B}]/[\mathrm{A}])[\mathrm{L}][\mathrm{A}]\} \\ &= K_0/\{1 + 1/K_{\mathrm{AB}}\} \end{aligned}$$

The enthalpy of ligand binding observed under such circumstances will include a contribution from the heat of isomerisation from B to A ($-\Delta H_{\mathrm{AB}}$) of that fraction of **3**, ($1 + 1/K_{\mathrm{AB}}$), originally in form B prior to binding.

Observed enthalpy:

$$\begin{aligned} \Delta H_{\mathrm{obs}} &= \Delta H_0 - \Delta H_{\mathrm{AB}}/(1 + 1/K_{\mathrm{AB}}) \\ &= \Delta H_0 - \Delta H_{\mathrm{AB}}/\{1 + \exp(-\Delta S_{\mathrm{AB}}/R).\exp(\Delta H_{\mathrm{AB}}/RT)\} \\ &\quad \text{using } \Delta G_{\mathrm{AB}} = -RT.\ln K_{\mathrm{AB}} = \Delta H_{\mathrm{AB}} - T.\Delta S_{\mathrm{AB}} \end{aligned} \quad (1)$$

The same expression (eqn. 1) can also be obtained rigorously by use of the van't Hoff relation: $\Delta H_{\mathrm{obs}} = -R.\mathrm{d}\ln K_{\mathrm{obs}}/\mathrm{d}(1/T)$

This equation (eqn. 1) adequately represents the heats of binding observed for each binding site (Fig. 5) with thermodynamic parameters, obtained by non-linear regression, listed in Table 2. The enthalpies of isomerisation, A → B, ΔH_{AB} are negative in both cases, consistent with A being the higher enthalpy state, and are of similar magnitude. Interestingly, a qualitative estimation of this value can also be obtained from both experimental and theoretical studies on benzene dimers. Two independent laboratories have reported dissociation energies of the benzene dimers being in the order of 1.6 ± 0.2 kcal mol^{-1}[35] and 2.4 ± 0.4 kcal mol^{-1}.[36] Assuming the formation of eight π–π interactions in **3**, this would give an estimation of ΔH_{AB} between -12.8 ± 1.6 and -19.2 ± 3.2 kcal mol^{-1}, respectively. In addition, high level theoretical calculations have been able to propose interaction energies for both offset and T-shape benzene dimers, these being 1.91 and 1.77 kcal mol^{-1}, respectively.[37] Assuming the formation of four offset and four T-shape π–π stacking interactions in the limit case of highly ordered forms, this would give an estimated ΔH_{AB} of -14.7 kcal mol^{-1}. All these values fit qualitatively well with the ΔH_{AB} value obtained experimentally by ITC, thus providing support for the hypothesis proposed above. It cannot be ruled out that such an agreement may be fortuitous, especially bearing in mind the different solvation effects to be considered in the different model systems. However, even correct sign and order of magnitude agreement is encouraging.

Using eqn. 1 we are also able to estimate the thermodynamic parameters for the binding of **1** to the "open" form of **3** (state A) in the absence of conformational switching. The value of ΔH_0 is negative in both cases, showing that binding is exothermic once the enthalpy due to conformational strain is accounted for. Site 1 binding involves only a relatively small, but favourable entropic component. Binding to site 2, in contrast, is much more exothermic, but involves a large negative entropy component that significantly offsets this favourable enthalpy.

The above analysis has been based on the assumption of temperature dependent isomerisation (or conformational switch) of the cyclodextrin. However, algebraically we would obtain the same result if we were to assume that it is the ligand **1** undergoing the isomerisation and, indeed, we have shown conformational flexibility in **1** both in solution and crystal complexes. A more

Table 2 Thermodynamic parameters (25 °C) derived by fitting experimental ITC data to the conformational switch/isomerisation model (eqn. 1)

	Site 1	Site 2
ΔH_0/kcal mol^{-1}	−8.3 (±0.2)	−15.9 (±0.3)
$\Delta S_0{}^{\circ}$/cal mol^{-1} K^{-1}	4 (±1)	−35 (±2)
ΔH_{AB}/kcal mol^{-1}	−11.3 (±0.1)	−14.1 (±0.2)
ΔS_{AB}/cal mol^{-1} K^{-1}	−34.7 (±0.3)	−44.7 (±0.9)
$T_{\mathrm{m,AB}}$/°C[a]	53 (±8)	42 (±11)

[a] Mid-point temperature for B → A transition, $T_{\mathrm{m,AB}} = \Delta H_{\mathrm{AB}}/\Delta S_{\mathrm{AB}}$

comprehensive conformational switch model would allow for isomerisation in both cyclodextrin and ligand, without altering the overall form of the equations. However, crystal structures (Fig. 9) show that either form of rocuronium can occupy the cyclodextrin cavity and NMR studies in solution[27,28] indicate that the energy differences between the conformers of **1** are relatively small (*ca.* ±1 kcal mol^{-1}). As such, this would make relatively little contribution to the ΔH_{AB} estimated here, which we therefore might attribute predominantly to conformational changes in the cyclodextrin. This is further supported by the lack of these anomalous effects when **1** binds to **2** under otherwise identical conditions.

It is interesting that the same value of ΔH_{AB} serves to describe the thermodynamic behaviour of both weak and strong binding modes of **1** to **3**. This again may be coincidental, but does suggest that the same conformational switch is required for either mode of binding. Unfortunately we do not yet have any structural data for the weakly complexed form, so are unable to speculate further.

Conclusions

Based on our observations a simple hypothesis for the binding of **1** to **3** can be put forward. The free form of **3** exists in solution in an unsymmetric conformation with one of the glucose units on the ring twisted towards the cavity, pushing the attached phenyl ring through the cavity. We believe some π–π interaction is taking place that also hinders the entrance of **1** for binding to **3**. This we have termed the "closed" form. For **1** to enter the cavity, the π–π interactions need to be disrupted and the conformation of the cyclodextrin needs to change to provide enough space for **1** to enter the cavity. The energy required to do this is the first endothermic step observed in the ITC data. ITC experiments further show a temperature dependency of the enthalpies of binding, consistent with the fact that at a higher temperature the π–π interactions and general conformation of the cyclodextrin will be able to adopt a less hindered conformation for **1** to enter. We have termed this the "open" form. This dynamic behaviour is consistent with NMR data. In addition, X-ray crystallography has provided unique evidence of the fact that the conformation of ring A in **1** can easily switch between a chair and a flattened twist-boat conformation, thus facilitating the entrance of **1** into **3**. The wealth of experimental data provided here supports the conformational switches experienced by **1** and **3** and represents a clear example of the recognition and mutual induced fit between a host (**3**) and its guest (**1**).

The studies reported here illustrate some of the complexities that can arise in both the design and analysis of even quite simple (apparently) host–guest systems, especially when significant conformational mobility is allowed. However, using this as a model we hope to improve understanding of the general receptor–ligand interactions required for efficient encapsulation between organic guest molecules and cyclodextrins. This will aid in the future design and development of cyclodextrins which complex with other biologically important molecules, pharmaceuticals and metabolites.

Experimental

Materials

The modified cyclodextrins (6-perdeoxy-6-per(4-carboxyphenyl)thio-γ-cyclodextrin sodium salt **3** and 6-perdeoxy-6-per(2-carboxyethyl)thio-γ-cyclodextrin sodium salt **2** were prepared following literature procedures.[16,12] Rocuronium bromide **1** is an Organon product and was supplied internally. The buffer used throughout was 50 mM sodium phosphate, pH 7.0, and sample concentrations were determined by weight.

ITC

Isothermal titration calorimetry experiments to measure the binding of ligands to cyclodextrins were done at 10–40 °C using a Microcal VP-ITC titration microcalorimeter following standard instrumental procedures[38,39] with a 250 μL injection syringe and 320 rpm stirring. Cyclodextrins and ligands were dissolved in the same buffer and degassed gently immediately before use. A typical binding experiment involved 25 × 10 μL injections of ligand solution (typically around 1.5 mM concentration) into the ITC cell (*ca.* 1.4 mL active volume) containing cyclodextrin (0.05–0.1 mM). The same experiments were performed in reverse, with cyclodextrin in the injection syringe and ligand in the cell. Control experiments were performed under identical conditions by injection of ligand or cyclodextrins into buffer alone (to correct for heats of ligand dilution) and injection of buffer into the complex mix (to check for heats of dilution of the complex, usually negligible). Integrated heat effects, after correction for heats of dilution, were analysed by non-linear regression in terms of a sequential two-site binding model using the standard Microcal Origin software package (other binding models failed to give satisfactory fits to these data). Other thermodynamic quantities were calculated using standard expressions: $\Delta G^\circ = -RT.\ln K = \Delta H^\circ - T.\Delta S^\circ$ (1 cal = 4.184 J).

UV/fluorescence spectroscopy

UV spectra of **3** in aqueous buffer solution were determined using a Shimadzu UV-1601 instrument with 1 cm pathlength quartz cuvettes, thermostatted at 25 °C. Fluorescence emission and excitation spectra were determined on the same samples using a Spex Fluoromax instrument with 5 nm slits, with 1 cm pathlength quartz fluorimeter cuvettes, thermostatted at 25 °C. Cyclodextrin concentrations were typically around 2 μM, giving an absorbance less than 0.2 at λ_{exc} to avoid inner filter effects. Fluorescence titration curves were obtained by adding small volumes (10–100 μL) of stock solutions of **1** , made up in the same cyclodextrin–buffer mixture, to avoid dilution effects. Data were fitted to standard hyperbolic binding curves using Microcal Origin software.

NMR

All NMR experiments were carried out on a Bruker DRX 400 spectrometer operating at 400.13 MHz for ^{1}H and 100.61 MHz for ^{13}C. The sample for the variable temperature spectra was 30 mg of **3** in 500 μL of D_2O with CH_3CN as an internal reference. 13 mg of **3** in 500 μL was used for the HSQC ^{1}H–^{13}C correlation spectrum[40] with CH_3CN as an internal reference (δ = ^{1}H 2.06, ^{13}C 1.47 ppm) for both ^{1}H and ^{13}C chemical shifts. The samples for the stack plot of ^{1}H spectra of **3**, **1** and their 1 : 1 mixture were 5 mM for **3**, 1 mM for both **1** and the mixture, and were dissolved in pH 7.5 phosphate buffered D_2O. 1D ^{1}H (0–80 °C) spectra were recorded with 64 scans and 32 K data points and processed by zero filling to 64 K data points. The stack plot spectra were recorded with 64 scans, presaturation of the water signal, 32 K data points and processed by zero filling to 64 K data points. The 2D HSQC spectrum was recorded with 80 scans with 2 K × 256 processed to a 2 K × 512 data matrix. The temperature control of samples was achieved using a Bruker BVT 3000 heater unit and a Bruker BCU 05 refrigerator unit.

Crystallography

6-Perdeoxy-6-per(4-carboxyphenyl)thio-γ-cyclodextrin sodium salt. The crystal structure of **3** arose from an unsuccessful attempt to record the crystal structure of the [**3**–**1**] complex.

A 1 : 1 mixture of **3** (512 mg) and **1** (122 mg) was suspended in hot (~80 °C) DMF and water added to the point of solution. This was then allowed to cool slowly over a period of 6 h then cooled on ice. The resulting solid (270 mg) was recrystallised by dissolving 155 mg in a 1 : 1 mixture of DMF:H_2O (7 mL)

and placed in a jar with DMF containing a few drops of H_2O and allowed to diffuse over a few days. The resulting crystals demonstrated the presence of **3** alone.

$C_{114}H_{118}Na_8O_{57.5}S_8$, $M = 2848.48$, crystal size 0.18 × 0.08 × 0.08 mm, tetragonal, $I4$, $a = 23.135(2)$ Å, $c = 31.904(3)$ Å, $V = 17075(3)$ Å^3, $Z = 4$, $r_{calcd} = 1.108$ g cm^{-3}; synchrotron radiation (CCLRC Daresbury Laboratory, Station 9.8, silicon monochromator, $\lambda = 0.6883$ Å), $\mu = 0.198$ mm^{-1}, $T = 150(2)$ K. 37397 data (7490 unique, $R_{int} = 0.0335$, $2.00 < \theta < 19.00°$), were collected on a Bruker AXS SMART CCD diffractometer using narrow frames and were corrected semiempirically for absorption and incident beam decay (transmission 0.9653–0.9844). The structure was solved by direct methods and refined by full-matrix least squares on F^2 values of all data (G. M. Sheldrick, SHELXTL, Bruker AXS, Madison WI, 1998, Version 5.10) to give $wR = \{\Sigma[w(F_o^2-F_c^2)^2]/\Sigma w(F_o^2)^2]\}^{1/2} = 0.3776$, conventional $R = 0.1601$ for F values of 5760 reflections with $F_o^2 > 2\sigma(F_o^2)$, $S = 2.830$ for 755 parameters. Residual electron density extremes were 0.709 and −0.591 eÅ^{-3}.

6-Perdeoxy-6-per(4-carboxyphenyl)thio-γ-cyclodextrin sodium salt–rocuronium bromide complex. A 1 : 1.6 mixture of **3** (256 mg) and **1** (97 mg) was suspended in DMF (4 mL), heated to ~80 °C and water (2.4 mL) added until dissolution was achieved. The solution was then allowed to cool very slowly by placing in a warm oven giving needle/rosette crystals. These have an NMR spectrum consistent with a 1 : 1 complex and were submitted for X-ray study without further washing.

$C_{136}H_{191}N_2Na_7O_{69}S_8$, $M = 3375.32$, crystal size 0.24 × 0.08 × 0.06 mm, monoclinic, $P2_1$, $a = 25.938(2)$ Å, $b = 31.856(2)$, $c = 26.526(2)$ Å, $\beta = 106.746(2)°$, $V = 20988(2)$ Å^3, $Z = 4$, $r_{calcd} = 1.068$ g cm^{-3}; synchrotron radiation (CCLRC Daresbury Laboratory, Station 9.8, silicon monochromator, $\lambda = 0.6883$ Å), $\mu = 0.172$ mm^{-1}, $T = 150(2)$ K. 67469 data (25027 unique, $R_{int} = 0.0520$, $2.244 < \theta < 22.493°$), were collected on a Bruker AXS SMART CCD diffractometer using narrow frames and were corrected semiempirically for absorption and incident beam decay (transmission 0.9599–0.9897). The structure was solved by direct methods and refined by full-matrix least squares on F^2 values of all data (G. M. Sheldrick, SHELXTL, Bruker AXS, Madison WI, 1998, Version 5.10) to give $wR = \{\Sigma[w(F_o^2-F_c^2)^2]/\Sigma w(F_o^2)^2]\}^{1/2} = 0.4263$, conventional $R = 0.1794$ for F values of 18 175 reflections with $F_o^2 > 2\sigma(F_o^2)$, $S = 3.099$ for 2828 parameters. Residual electron density extremes were 1.406 and −0.668 eÅ^{-3}.

Supporting information available

Crystallographic data in CIF format are available.

Acknowledgements

We thank J. K. Clark for technical expertise in growing adequate crystals of 6-perdeoxy-6-per(4-carboxyphenyl)thio-γ-cyclodextrin sodium salt, as the complex and free entity. We also appreciate G. Wishart for graphical assistance.

References

1 J. M. Hunter, *N. Engl. J. Med.*, 1995, **332**, 1691–1699.
2 D. M. Fisher, *Am. J. Health Syst. Pharm.*, 1995, **56**(11), 54–59 (Suppl. 1).
3 D. C. Rees and D. R. Hill, *Annu. Rep. Med. Chem.*, 1996, **31**, 41–50.
4 J. J. Saverese, J. E. Caldwell, C. A. Lien and R. D. Miller, in *Anesthesia*, ed. R. D. Miller, Churchill-Livingston, Philadelphia, 2000, pp. 412–490.
5 D. R. Bevan, F. Donati and A. F. Kopman, *Anesthesiology*, 1992, **77**, 785–805.
6 H. Berg, J. Roed, J. Viby-Mogensen, C. R. Mogensen, J. Engbaek, L. T. Skovgaard and J. J. Krintel, *Acta Anaesthesiol. Scand.*, 1997, **41**, 1095–1103.
7 N. J. N. Harper and B. J. Pollard, in *Muscle Relaxants in Anaesthesia*, ed. N. J. N. Harper and B. J. Pollard, Edward Arnold, London, 1995, pp. 135–155.
8 A. Bom, J. K. Clark and R. Palin, *Curr. Opin. Drug Discovery Dev.*, 2002, **5**, 793–800.
9 M. Endou, Y. Tanito and F. Okumura, *J. Pharmacol. Exp. Ther.*, 1997, **282**, 1480–1486.
10 A. Bom, A. Muir and D. C. Rees, PCT Int. Appl. WO 0112202 A2, 2001, *Chem. Abstr.*, 2001, **134**, 193457.
11 M.-Q. Zhang, R. Palin and D. J. Bennett, PCT Int. Appl. WO 0140316 A1, 2001, *Chem. Abstr.*, 2001, **135**, 29151.
12 J. M. Adam, J. D. Bennett, A. Bom, J. K. Clark, H. Feilden, E. J. Hutchinson, R. Palin, A. Prosser, D. C. Rees, G. M. Rosair, D. Stevenson, G. T. Tarver and M.-Q. Zhang, *J. Med. Chem.*, 2002, **45**, 1806–1816.
13 M.-Q. Zhang and D. C. Rees, *Expert Opin. Ther. Pat.*, 1999, **9**, 1697–1717.
14 A. Bom, M. Bradley, K. Cameron, J. K. Clark, J. van Egmond, H. Feilden, E. J. MacLean, A. Muir, R. Palin, D. C. Rees and M.-Q. Zhang, *Angew. Chem., Int. Ed.*, 2002, **41**, 256–270.
15 R. Palin, *12th RSC-SCI Medicinal Chemistry Symposium (part IV)*, 2003.
16 K. S. Cameron, J. K. Clark, A. Cooper, L. Fielding, R. Palin, S. J. Rutherford and M.-Q. Zhang, *Org. Lett.*, 2002, **4**, 3403–3406.
17 A. Cooper and K. E. McAuley-Hecht, *Philos. Trans. R. Soc. London, A*, 1993, **345**, 23–35.
18 D. McPhail and A. Cooper, *J. Chem. Soc., Faraday Trans.*, 1997, **93**, 2283–2289.
19 C. Clarke, R. J. Woods, J. Gluska, A. Cooper, M. A. Nutley and G. J. Boons, *J. Am. Chem. Soc.*, 2001, **123**, 12238–12247.
20 A. Cooper, C. M. Johnson, J. H. Lakey and M. Nöllmann, *Biophys. Chem.*, 2001, **93**, 215–230.
21 L. Fielding, *Tetrahedron*, 2000, **56**, 6151–6170.
22 C. A. Hunter and J. K. M. Sanders, *J. Am. Chem. Soc.*, 1990, **112**, 5525–5534.
23 D. S. Savage, A. F. Cameron, G. Ferguson, C. Hannaway and I. R. Mackay, *J. Chem. Soc. B*, 1971, 410–415.
24 H. Kooijman, V. J. van Geerestein, P. van der Sluis, J. A. Kanters, J. Kroon, C. W. Funke and J. Kelder, *J. Chem. Soc. Perkin Trans. 2*, 1991, 1581–1586.
25 H. Kooijman, J. Kelder, J. A. Kanters, A. J. M. Duisenberg and J. Kroon, *J. Chem. Soc. Perkin Trans. 2*, 1996, 2133–2140.
26 L. Fielding, *Magn. Reson. Chem.*, 1998, **36**, 387–397.
27 L. Fielding and G. H. Grant, *J. Am. Chem. Soc.*, 1991, **113**, 9785–9790.
28 L. Fielding and G. H. Grant, *J. Am. Chem. Soc.*, 1993, **115**, 1902–1907.
29 Z. Galdecki, P. Grochulski, Z. Wawrzak, W. L. Duax and P. D. Strong, *J. Crystallogr. Spectrosc. Res.*, 1989, **19**, 561–568.
30 K. Harata, *Chem. Lett.*, 1984, **4**, 641–644.
31 K. Harata, *Bull. Chem. Soc. Jpn*, 1987, **60**, 2763–2767.
32 J. Ding, T. Steiner, V. Zabel, B. Hingerty, S. A. Mason and W. Saenger, *J. Am. Chem. Soc.*, 1991, **113**, 8081–8089.
33 W. Saenger, J. Jacob, K. Gessler, T. Steiner, D. Hoffmann, H. Sanbe, K. Koizumi, S. Smith and T. Takaha, *Chem. Rev.*, 1998, **98**, 1787–1802.
34 H. Dodziuk, *J. Mol. Struct.*, 2002, 33–45.
35 H. Krause, B. Ernstberger and H. J. Neusser, *Chem. Phys. Lett.*, 1991, **184**, 411–417.
36 J. R. Grover, E. A. Walters and E. T. Hui, *J. Phys. Chem.*, 1987, **91**, 3233–3237.
37 F. Tran, J. Weber and T. A. Wesolowski, *Helv. Chim. Acta*, 2001, **84**, 1489–1503.
38 T. Wiseman, S. Williston, J. F. Brandts and L.-N. Lin, *Anal. Biochem.*, 1989, **179**, 131–137.
39 A. Cooper and C. M. Johnson, in *Microscopy, Optical Spectroscopy, and Macroscopic Techniques, Methods in Molecular Biology,* ed. C. Jones, B. Mulloy and A. H. Thomas, Humana Press, Totowa, NJ, 1994, vol. 22, pp. 137–150.
40 L. E. Kay, P. Keifer and T. Saarinen, *J. Am. Chem. Soc.*, 1992, **114**, 10663–10665.